State of Charge Estimation of Lithium Sulfur Batteries using Sliding Mode Observer

Srinivasan Munisamy
Advanced Vehicle Enginnering Centre, SATM
Cranfield University
Cranfield, Bedfordshire, UK
ORCID **0000-0003-3497-8149**

Wenxuan Wu
Advanced Vehicle Enginnering centre
Cranfield University
Cranfield, Bedforshire, UK

***Abstract*—The lithium-sulfur (Li-S) batteries are high energy storage systems that can be used for electric grid and solar power air vehicle applications. Modelling and the state of charge (SOC) estimation of discharging Li-S are highly challenging than other batteries as the discharge voltage of Li-S batteries has highly nonlinear and typical characteristics than the Lithium-Ion batteries. For Li-S battery SOC estimation, literature has proposed filters and machine learning techniques, but no literature on sliding mode observer (SMO). This paper presents the SMO for discharging Li-S SOC estimation and compares it to the extended Kalman filter (EKF). Both estimators use a first-order equivalent circuit network (ECN) model of Li-S cell parameters given in the literature. The performance of such ECN model based SOC estimators influenced by the Q- uncertainty, which is a perturbation in the form of process noise state-space model. Therefore, this work studies an optimal trade-off characteristics of SMO and EKF over the Q-uncertainty. With constant and mixed-amplitude pulse load current sequences, numerical simulation has performed. Simulation results illustrate that the SMO is optimal, converges to the true SOC than the EKF when the perturbation increased.**

Keywords—Battery energy storage, nonlinear filters, Lithium-sulfur batteries, state of charge, sliding mode observer.

I. INTRODUCTION

Recently, the battery energy storage systems (BESSs) have been active research owing their applications including electric grids and vehicles. There are different battery technologies such as Lithium-Ion(Li-Ion), lithium-sulfur, lithium-air and so on. Compared commercialized well-known Li-Ion, the Li-S batteries have some good features [1] such as higher energy storage capabilities, safety, lesser-weight and low cost. Due to such features, the Li-S Such batteries can be used as energy storage systems in long-range vehicles including solar-powered small aircraft [2]. Through the battery management systems (BMSs), the SOC plays significant role for the energy or power optimization, control and to improve safety of batteries. The BESSs of such applications require an appropriate algorithm to evaluate the state of charge (SOC) of the batteries.

The SOC estimation of discharging Li-S batteries is challenging as the open circuit voltage (OCV) of Li-S batteries has deep-dive high-plateau and flatten, poorly-observable low-plateau behavior [1,3]. This behavior is different than the traditional Li-Ion batteries. Literature has proposed a couple of SOC estimators, for instance, the machine learning approaches such as nonlinear filters [4,5,6], adaptive nuero-fuzzy inference system (ANFIS) [7], and Support Vector Machine (SVM) [8],. But there is not literature on sliding mode observer (SMO) based SOC estimation for Li-S batteries though SMO were widely used for SOC estimation of Li-Ion [9-11]. This paper fulfills such literature gap by designing a sliding mode observer for Li-S battery cell.

First, the SMO is designed for a deterministic first-order equivalent circuit network (ECN) model of discharging Li-S batteries. Next, on top of that, the perturbation is introduced into ECN model to study the robustness of the SMO. It is assumed that perturbation is Gaussian noise and it is bounded with known variance. The process noise is referred as Q-uncertainty. According to voltage and parameter characteristics, the gains of SMO SOC estimator are chosen. The stability of the SMO can be studied by the Lyapunov error function. Applying constant and dynamic load current, the performance of SMO is analyzed. The SMO's performance is compared to the traditional extended Kalman filter (EKF). While designing EKF, the discrete-time model is used, whereas a continuous-time model is used for SMO. However, both SMO based SOC estimator uses ECN model and prediction error minimization based parameterization available in the public domain [12]. Simulation results show that compared to the EKF the SMO is robust and the accuracy in error is less than five percent for considered Q-uncertainty.

The rest of the paper is organized as follow: Section II studies the modelling complexity and SOC problem formulation of discharging Li-S battery cell. The EKF is presented section III, and the SMO is studied in section IV. Simulation results and their discussions are given in section V. Finally, section VI presents the conclusions and future works of this paper.

II. LI-S BATTERY DISCHARGE VOLTAGE

A. Deterministic ECN Model

This section describes the deterministic state-space model of discharging Li-S battery model derived from ECN model given in Fig 1. Such model reported in the literature [12]. The modeling is repeated here because to contrast the discharge voltage of Li-S battery from the voltage of Li-Ion battery and to extend the deterministic model to uncertainty model.

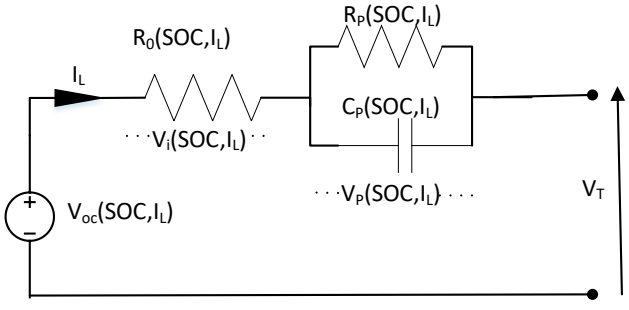

Fig.1 A first-order ECN model represents a Li-S battery cell.

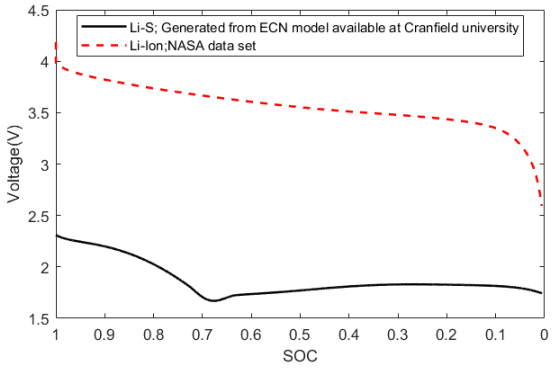

Fig.2 Li-S vs Li-Ion: voltage comparison of Li-S and Li-Ion batteries

Though the model is deterministic, the modeling complexity of Li-S batteries is higher than the transition Li-Ion because the typical voltage characteristic. Fig 2 compares the voltage characteristics of typical Li-S and Li-Ion batteries. In Fig 2, the solid-blank line indicates the measured voltage of 2Ah Li-Ion battery given in [13], and the red-dashed line represents the voltage of 2.72Ah Li-S battery that generated from the SIMULINK model [12]. These voltages are battery response to 2A constant current and begin from maximum voltage and end at the curt-off voltage of respective battery cell. It is an evident that the voltage of Li-S has a deep-dive high plateau during 0 to 1500s and a flat-in nature low plateau from 1500s to 5000s approximately. The high- and low-plateau have joined with a sharp curve, which is an additional complexity in the modeling of Li-S batteries. Therefore, the output or measurement model of state-space for discharging Li-S batteries is quite different from the traditional one. Such difference is explained with an example in rest of this section. The state-space model is written as

$$\dot{x}(\mathrm{t}) = f_c(x(t), \theta_b(x_1(t)), I_{\mathrm{L}}(t)); \quad x(t_0) \tag{1}$$

$$y(t) = V_T = h_c(x(t), \theta_b(x_1(t)), I_{\mathrm{L}}(t)) \tag{2}$$

Where $x(t) = \begin{bmatrix} SOC \\ V_P \end{bmatrix} = \begin{bmatrix} x_1(t) \\ x_2(t) \end{bmatrix}$ is a state vector, $\dot{x}(\mathrm{t})$ is the first derivative of $x(t)$, and $\theta_b(x_1(t))$ denotes parameters of ECN model, which are functions of SOC. The deterministic SOC is evaluated from the following first-order differential equation

$$\dot{x}_1(t) = \frac{-I_L}{3600\, Q_{\mathrm{cap}}}; \quad x_1(t_0) \tag{3}$$

where $\dot{x}_1(\mathrm{t})$ is the first derivative of SOC at time t, $x_1(t_0)$ is the initial SOC at time t_0, the Q_{cap} is the capacity of the battery, and I_{L} is the load current or current taken out from the battery. The dynamic behavior of polarization voltage, V_P across the 1RC network is expressed as

$$\dot{x}_2(t) = \frac{-1}{C_{\mathrm{P}}(x_1(t))R_{\mathrm{P}}(x_1(t))} x_2(t) + \frac{I_{\mathrm{L}}}{C_{\mathrm{P}}(x_1(t))}; x_2(0) \tag{4}$$

where $R_{\mathrm{P}}(x_1(t))$ and $C_{\mathrm{P}}(x_1(t))$ are resistor and capacitor of 1RC branch, respectively.

From Fig 1, the battery terminal voltage, $V_T(\mathrm{t})$, is expressed as

$$V_T(\mathrm{t}) = V_{\mathrm{oc}}(x_1) - x_2(\mathrm{t}) - I_{\mathrm{L}} R_{\mathrm{o}}(x_1) \tag{5}$$

where $V_{\mathrm{oc}}(x_1)$ is the open circuit voltage of the battery, $x_2(\mathrm{t})$ denotes polarization voltage, and $R_{\mathrm{o}}(x_1)$ is the Ohmic resistance of the battery. Unlike the parameters of lithium-ion, the $V_{\mathrm{oc}}(x_1)$ and $R_{\mathrm{o}}(x_1)$ of Li-S battery have high and low-plateau are joined by a partial sinusoidal function (PSF) [4] as follow:

$$V_{OC}(x_1) = \gamma(x_1(t))V_{oc,high}(x_1(t)) + (1 - \gamma(x_1(t)))V_{oc,low}(x_1(t)) \tag{6}$$

$$R_o(x_1) = \gamma(x_1(t))R_{o,high}(x_1(t)) + (1 - \gamma(x_1(t)))R_{o,low}(x_1(t)) \tag{7}$$

where

$$V_{oc,high}(x_1(t)) = p_{1,Vohi}{x_1}^n + p_{2,vohi}{x_1}^{n-1} + \cdots + p_{n,vohi}\, x_1 + p_{n+1,vohi} \tag{8}$$

$$V_{oc,low}(x_1(t)) = p_{1,volo}{x_1}^n + p_{2,volo}{x_1}^{n-1} + \cdots + p_{n,volo}\, x_1 + p_{n+1,volo} \tag{9}$$

$$R_{o,high}(x_1(t)) = p_{1,Rohi}{x_1}^n + p_{2,Rohi}{x_1}^{n-1} + \cdots + p_{n,Rohi}\, x_1 + p_{n+1,Rohi} \tag{10}$$

$$R_{o,low}(x_1(t)) = p_{1,Rolo}{x_1}^n + p_{2,Rolo}{x_1}^{n-1} + \cdots + p_{n,Rolo}\, x_1 + p_{n+1,Rolo} \tag{11}$$

and

$$\gamma(x_1(t)) = \begin{cases} 0, & if\ L_P \\ f_{PSF}(x_1(t)), & if\ J_{trans} \\ 1, & if\ H_P \end{cases} \tag{12}$$

with

$$f_{PSF}(x_1(t)) = 0.5 + 0.5\, sin(2(5\pi)(x_1 - \mathrm{m})) \tag{13}$$

$$L_P\colon 0 \le x_1 \le \mathrm{a}$$
$$J_{trans}\colon \mathrm{a} < x_1 < \mathrm{b} \tag{14}$$
$$H_P\colon \mathrm{b} \le x_1 \le 1$$

In (8)-(11), the $p_{1,..}$, $p_{2,...}$ and p_{n+1} are the coefficients of nth order polynomial for each parameters.

According to Table 2 of [3], the parameters of REVB's Li-S cell of 2.72 Ah at 20°C are written as:

$$V_{oc,high}(x_1(t)) = 108.1{x_1}^5 - 361.13{x_1}^4 + 444.73{x_1}^3 - 238.18{x_1}^2 + 47.03x_1 + 1.88 \tag{15}$$

$$V_{oc,low}(x_1(t)) = -752.62{x_1}^8 + 2085.66{x_1}^7 - 2392.87{x_1}^6 + 1466.98{x_1}^5 - 517.42{x_1}^4 + 105.21{x_1}^3 - 11.69{x_1}^2 + 0.62x_1 + 2.1 \tag{16}$$

$$R_{o,high}(x_1) = -1300.2{x_1}^6 + 6470.07{x_1}^5 - 13362.95{x_1}^4 + 14656.94{x_1}^3 - 9000.23{x_1}^2 + 2931.67x_1 - 395.2() \tag{17}$$

$$R_{o,low}(x_1) = 12.96{x_1}^6 - 28.54{x_1}^5 + 25.46{x_1}^4 - 11.65{x_1}^3 + 3.09{x_1}^2 - 0.42x_1 + 0.11 \tag{18}$$

$$R_P(x_1) = 140.636{x_1}^9 - 613.186{x_1}^8 + 1088.525{x_1}^7 - 1005.911{x_1}^6 + 512.386{x_1}^5 - 139.174{x_1}^4 + 16.887{x_1}^3 - 0.011{x_1}^2 - 0.223x_1 + 0.074 \tag{19}$$

$$C_P(x_1) = 89414.28{x_1}^5 - 113090.73{x_1}^4 + 25401.28{x_1}^3 + 15392.5{x_1}^2 - 3017.3x_1 + 306.23 \tag{20}$$

$$f_{PSF}(x_1(t)) = 0.5 + 0.5\, sin(2(5\pi)(x_1 - 0.68)) \tag{21}$$

$$L_P\colon 0 \le x_1 \le 0.63$$
$$J_{trans}\colon 0.63 < x_1 < 0.73 \tag{22}$$
$$H_P\colon 0.73 \le x_1 \le 1$$

These parameters are used to characterize the discharging Li-S cell from the deterministic model (1)-(2) with two different types of load current. When applied mixed-amplitude pulse current sequence and assumed that the initial SOC was one, the Li-S cell have the typical high- and low-plateau voltage characteristic, as shown by Fig 3(a). Fig 3(b) shows the mixed-amplitude pulse current sequence. Fig 3(c) and Fig 3(d) denote the SOC and the dynamic polarization voltage of cell to the pulse current, respectively. Fig 4 shows a zoomed section of the voltage to current pulses with different amplitudes such as 0.5A(0.2C), 1A(0.4C) and 1.5A(0.55C) are considered. This exhibits the impact of polarization voltage on the dynamic voltage behavior. Therefore, the SOC

estimators need a first of ECN model and its parameters are shown by Fig 3(e)-(h) .

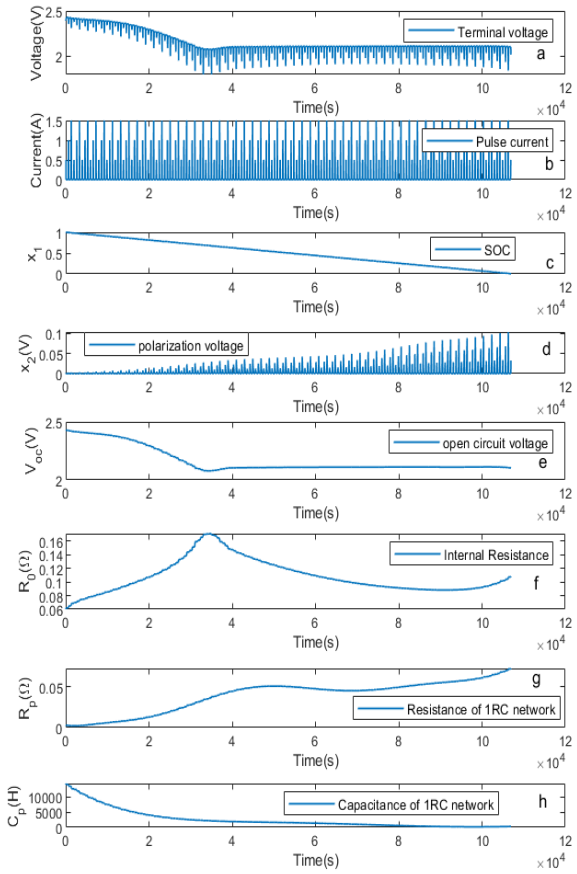

Fig.3 Characteristics of REVB's Li-S cell to mixed-pulse current: (a)voltage; (b) current; (c) True SOC, x_1; (d) True x_2 ; (e). $V_{OC}(x_1)$; (f). $R_O(x_1)$; (g). $R_P(x_1)$; (h). $C_P(x_1)$..

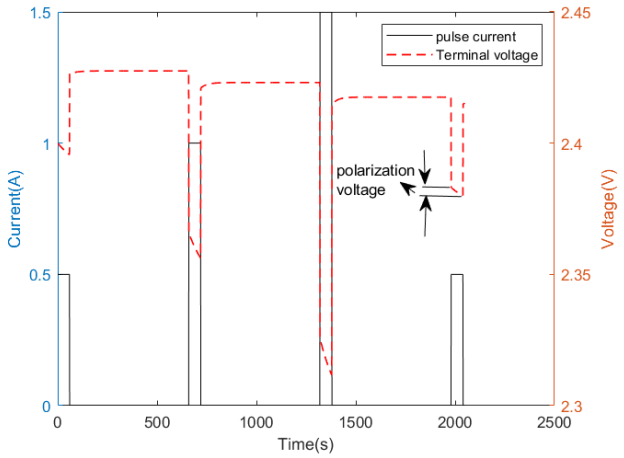

Fig. 4. Zoomed a section of Voltage of Li-S to the pulse current

B. *Model with Pertubation*

Due to unknown modeling error and sensor noise, the state and measurement models have perturbations. Such perturbations can be modelled as noise with known mean and variance. In this work, it is assumed the modelling error and sensor noise are Gaussian noise. The is assumed that the actual noise variance of batteries varies in the form of additive noise of the state-space model as

$$\dot{x}(\mathrm{t}) = f_c(x(t), \theta_b, u(t)) + w_a(t); x(t_0) \quad (23)$$

$$y = h_c\big((t), \theta_b, u(t)\big) + v_a(t) \quad (24)$$

Where $w_a(t) \sim N(0, Q_a)$ and $v_a(t) \sim N(0, R_a)$ are they are the independent and identically distributed Gaussian noises, The noise $w_a(t)$ represents the unknown modelling error in the SOC model (3) and polarization voltage model (4). Furthermore the process noise assumes that the state variables are not correlated one to another. Therefore the process noise covariance Q_a can be expressed as

$$Q_a = \begin{bmatrix} Q_{soc} & 0 \\ 0 & Q_{vp} \end{bmatrix} \quad (25)$$

in which Q_{soc} and Q_{vp} (V^2) denote the variances of noise in the SOC and the polarization voltage, respectively. The R_a denotes the covariance of sensor noise. Both $w_a(t)$ and $v_a(t)$ are treated as perturbations that bounded with known variance, of process and measurement model respectively. These statistical parameters Q_a and R_a are uncertain, not known exactly when batteries are used for applications like EVs. Fig 5 shows a behavior of perturbed and unperturbed state (Fig 5c shows x_2) and output variable (Fig. 5b show terminal voltage), and parameter (Fig 5d shows V_{oc}) of Li-S cell that generated from the ECN model when pulse current is applied, Fig 5a.

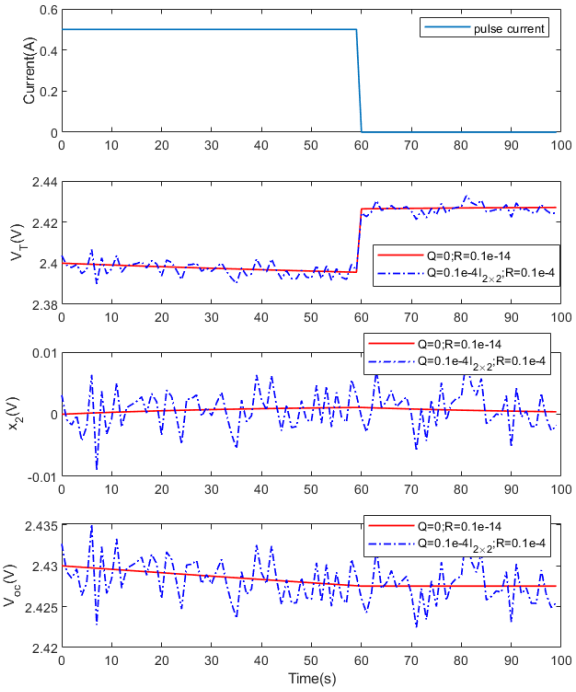

Fig.5 Perturbation on Li-S cell model when pulse current is applied (a) pulse current; (b) terminal voltage with noise; (c) x_2 ; (d). $V_{OC}(x_1)$

III. EKF BASED SOC ESTIMATOR

The EKF uses discrete state-space model. The discretized version of (23)-(24) is written as:

$$x_{k+1} = \mathrm{f}_d(x_k, \theta_{b,k}, I_{L,k}) + w_k \quad (27)$$

$$y_k = h_d(x_k, \theta_{b,k}, I_{L,k}) + v_k \quad (28)$$

where k is the sampling time index,

$$\mathrm{f}_d(x_k,\theta_k,I_{L,k}) = \begin{bmatrix} \mathrm{f}_{d,1}(x_{1,k},I_{L,k}) \\ \mathrm{f}_{d,2}(x_k,,\theta_k,I_{L,k}) \end{bmatrix} = \begin{bmatrix} x_{1,k} - \frac{\Delta t * I_{L,k}}{3600 * Q_{cap}} \\ x_{2,k} - \frac{\Delta t * x_{2,k}}{C_P(x_{1,k}) R_P(x_{1,k})} + \frac{\Delta t * I_{L,k}}{C_P(x_{1,k})} \end{bmatrix}, \quad (29)$$

$$\mathrm{h}_d(x_k,\theta_k,u_k) = V_{oc}(x_{1,k}) - x_{2,k} - R_P(x_{1,k}) I_{L,k} \quad (30)$$

w_k and v_k are the process and measurement noise.. Δt is sample time. $x_k = \begin{bmatrix} x_{1,k} \\ x_{2,k} \end{bmatrix}$ and $I_{L,k}$ are the discrete state and input same as the continuous model. The parameters of the discrete model are the same as the parameters of the continuous model. In the EKF, the following Jacobian matrices are used:

$$A_k = \frac{\partial \mathrm{f}_d(x_k,I_{L,k})}{\partial x_k} = \begin{bmatrix} 1 & 0 \\ \frac{\partial \mathrm{f}_{d,2}(x_k,I_{L,k})}{\partial x_{1,k}} & \frac{\partial \mathrm{f}_{2,k}(x_k,I_{L,k})}{\partial x_{2,k}} \end{bmatrix} \quad (30)$$

$$B_k = \frac{\partial \mathrm{f}_d(x_k,I_{L,k})}{\partial I_{L,k}} = \begin{bmatrix} -\frac{\Delta t}{3600 * Q_{cap}} \\ \frac{\Delta t}{C_P(x_{1,k})} \end{bmatrix} \quad (31)$$

$$C_k = \frac{\partial \mathrm{h}_d(x_k,I_{L,k})}{\partial x_k} = \begin{bmatrix} \frac{\partial h_d(x_k,I_{L,k})}{\partial x_{1,k}} & -1 \end{bmatrix} \quad (32)$$

$$D_k = \frac{\partial \mathrm{h}_d(x_k,I_{L,k})}{\partial I_{L,k}} = \begin{bmatrix} -R_0(x_{1,k}) \end{bmatrix} \quad (33)$$

The EKF algorithm includes five steps predicted state estimate, predicted covariance estimate, near-optimal Kalman gain calculation, state estimate update, and covariance of the state estimate. '-' and '+' at the top-right corner of each variable means before (prior) or after (posterior) the calculation [4]. Before the algorithm, the initial condition of the EKF algorithm is set as Eq. (33):

$$k = 0$$
$$\hat{x}_0^+ = \begin{bmatrix} 1 \\ 0 \end{bmatrix}$$
$$P_0^+ = \begin{bmatrix} 10 & 0 \\ 0 & 10 \end{bmatrix} \quad (33)$$

k in EKF is the step. $\hat{x}_k^-$ and $\hat{x}_k^+$ are the prior and posterior state estimates. P_k^- and P_k^+ are the prior and posterior error covariances. K_k is the Kalman gain. The EKF follows main steps:

The predicted state estimate:

$$\hat{x}_k^- = A_{k-1}\hat{x}_{k-1} + B_{k-1} I_{L,k-1} \quad (34)$$

The Predicted covariance estimate:

$$P_k^- = A_{k-1} P_{k-1}^+ A_{k-1}^T + Q \quad (35)$$

Q is the process noise. Q is the same as Δf_1 in SMO.

Near-optimal Kalman gain calculation:

$$K_k = P_k^- C_k^T (C_k P_k^- C_k^T + R)^{-1} \quad (36)$$

R is the measurement noise. R is the same as Δf_3 in SMO. In the result section, both Q and R will be changed to test the robustness.

State estimate update:

$$\hat{x}_k^+ = \hat{x}_k^- + K_k(y_k - C_k\hat{x}_k^- - D_k I_{L,k}) \quad (37)$$

The posterior states are estimated by Kalman gain, prior states and the measurement of terminal voltage y_k.

Covariance of the state estimate:

$$P_k^+ = (I - K_k C_k) P_k^- \quad (38)$$

After estimating covariance of the state, the five steps are finished, and a new loop will begin from (33) to (37). Finally, after all the data is processed, the loop finishes.

This work under grants European commission grant 814471e, and the Aerospace Technology Institute (ATI) and Innovate UK TS/P003818/1 and TS/R013780/1, respectively.

IV. SMO BASED SOC ESTIMATOR

Continuous-time state-space of Li-S discharge model (23)-(24) is considered for design sliding mode observer based SOC estimator. is designed For designing the sliding-mode observer and simulate the noise or perturbations, an equation of terminal voltage with uncertainty is given:

$$\mathrm{y(t)} = V_{\mathrm{oc}} - x_2(\mathrm{t}) - V_{\mathrm{L}} + \Delta y \quad (39)$$

Where $V_{\mathrm{L}} = R_o I_L$, and Δy is the bounded uncertainty of measurement, which is equal to $v_a(t)$ with known covariance R_a. The time derivative for the SOC with an assuming uncertainty is:

$$\dot{x}_1 = -\frac{I_{\mathrm{L}}}{3600 Q_{\mathrm{cap}}} + \Delta x_1 \quad (40)$$

Where Δx_1 is a bounded perturbation of the SOC, which is characterized as a Gaussian noise with known covariance Q_{soc}. Having $V_{\mathrm{L}} = R_o I_L$ and assuming no uncertainty in (39), the load current can be expressed as

$$I_{\mathrm{L}} = \frac{V_{\mathrm{oc}} - x_2(\mathrm{t}) - \mathrm{y(t)}}{R_o} \quad (41)$$

Substitution of (41) in (40) results the following first derivative of SOC :

$$\dot{x}_1(\mathrm{t}) = -\frac{V_{\mathrm{oc}} - x_2(\mathrm{t}) - \mathrm{y(t)}}{3600 Q_{\mathrm{cap}} R_{\mathrm{o}}} + \Delta x_1 = a_1(\mathrm{y(t)} + x_2(\mathrm{t}) - V_{\mathrm{oc}}) + \Delta x_1 \quad (42)$$

where $a_1 = \frac{1}{3600 Q_{\mathrm{cap}} R_{\mathrm{o}}}$, and Δf_1 is the bounded uncertainty of the capacity term. The polarization voltage is written as:

$$\dot{x}_2(\mathrm{t}) = \frac{-1}{C_{\mathrm{p}} R_{\mathrm{p}}} x_2(\mathrm{t}) + \frac{I_{\mathrm{L}}}{C_{\mathrm{p}}} + \Delta x_2 = -a_2 x_2(\mathrm{t}) + b_1 I_{\mathrm{L}} + \Delta x_2 \quad (43)$$

which $a_2 = \frac{1}{C_{\mathrm{p}} R_{\mathrm{p}}}$, $b_1 = \frac{1}{C_{\mathrm{p}}}$, and Δx_2 is the uncertainty of the polarization voltage, which is characterized by Gaussian noise with Q_{vp}.

Now, let express dynamic response of measured battery terminal voltage by taking derivative of (39). Such first derivative output voltage can be expressed with bounded perturbation $\Delta\dot{y}$ as:

$$\dot{y}\,(\mathrm{t}) = \dot{V}_{oc} - \dot{x}_2(\mathrm{t}) - \frac{d}{dt}(I_{\mathrm{L}} R_{\mathrm{o}}) + \Delta\dot{y} \quad (44)$$

Considering a fast-sampling time the derivative of the terminal voltage $y\,(\mathrm{t})$ to the load current is negligible ($\frac{\Delta \mathrm{V_L(t)}}{\Delta I_{\mathrm{L}}} \approx 0$). Therefore, the (14) can be expressed as

$$\dot{y}\,(\mathrm{t}) = -\frac{I_{\mathrm{L}}}{3600 Q_{\mathrm{cap}}} + \frac{1}{C_{\mathrm{p}} R_{\mathrm{p}}} x_2(\mathrm{t}) - \frac{I_{\mathrm{L}}}{C_{\mathrm{p}}} + \Delta\dot{y} \quad (45)$$

Substitution of $x_2(\mathrm{t}) = V_{\mathrm{oc}} - \mathrm{y(t)} - I_{\mathrm{L}} R_{\mathrm{o}}$ in (45) results

$$\dot{y}\,(\mathrm{t}) = -\frac{I_{\mathrm{L}}}{3600 Q_{\mathrm{cap}}} + \frac{V_{\mathrm{oc}} - y(t) - I_{\mathrm{L}} R_{\mathrm{o}}}{C_{\mathrm{p}} R_{\mathrm{p}}} - \frac{I_{\mathrm{L}}}{C_{\mathrm{p}}} + \Delta\dot{y} = -a_2 y(t) + a_2 V_{\mathrm{oc}} - b_2 I_{\mathrm{L}} + \Delta\dot{y} \quad (46)$$

where $b_2 = \frac{1}{3600 Q_{\mathrm{cap}}} + \frac{1}{C_{\mathrm{p}}} + \frac{R_{\mathrm{o}}}{C_{\mathrm{p}} R_{\mathrm{p}}}$. since the observability matrix is full rank, the state vector can be estimated.

To estimate the terminal voltage (46), the SMO uses the following model:

$$\dot{\hat{y}} = -a_2\hat{y} + a_2\hat{V}_{oc} - b_2 I_{\mathrm{L}} + L_1 sgn(y(\mathrm{t}) - \hat{y}) \quad (47)$$

where L_1 is a positive gain of the terminal voltage SMO, the $\hat{y}$ and $\hat{V}_{oc}$ are the estimations of $y(t)$ and V_{oc}. After defining the error as $e_L = (y(\mathrm{t}) - \hat{y})$, the error dynamic equation of the terminal voltage can be expressed as:

$$\dot{e}_L(\mathrm{t}) = -a_2 e_L(\mathrm{t}) + a_2(V_{oc} - \hat{V}_{oc}) + \Delta\dot{y} - L_1 sgn(e_{\mathrm{L}}(t)) \quad (48)$$

where

$$sgn(e_{\mathrm{L}}(t)) = \begin{cases} 1, & e_{\mathrm{L}}(t)>0 \\ -1, & e_{\mathrm{L}}(t)<0 \end{cases} \quad (49)$$

It is assumed that the gain L_1 satisfies an inequality

$$L_1 > \left|a_2\left(V_{oc} - \hat{V}_{oc}\right) + \Delta\dot{y}\right| \quad (50)$$

The following Lyapunov function can be used to prove the error convergence:

$$\mathrm{V(e(t))} = \frac{1}{2}e_L^2(t). \quad (51)$$

In this work, the gain L_1 for considered Li-S cell's terminal voltage estimation is determined by

$$L_1 > \left|a_2\left(V_{oc} - \hat{V}_{oc}\right) + \Delta\dot{y}\right| \approx |\Delta\dot{y}| + 0.035 \quad (52)$$

This is according to the V_{oc} given in black solid-line of Fig. 2, perturbation in the measurement, and the maximum a_2 is 0.09842 by calculating the $\frac{1}{C_{\mathrm{p}}R_{\mathrm{p}}}$. When estimation of terminal voltage reaches the sliding surface, $\dot{e_{\mathrm{L}}}$ and e_{L} reaches to 0. According to the equivalent control method, i.e., $\frac{L_1}{a_2}sgn(e_L)$ is replaced by $\left\{\frac{L_1}{a_2}sgn(e_L)\right\}_{eq}$, the (52) can be written as an equivalent function as :

$$V_{\mathrm{oc}} - \hat{V}_{oc} = \left\{\frac{L_1}{a_2}sgn(e_L)\right\}_{eq}. \quad (53)$$

The sliding mode observer model of $\hat{x}_1(t)$ is written as :

$$\dot{\hat{x}}_1 = a_1\left(\hat{y} + \hat{x}_2 - \widehat{V_{\mathrm{oc}}}\right) + L_2 sgn(e_1) \quad (54)$$

Where $e_1 = x_1 - \hat{x}_1$ is an error between actual SOC and estimated SOC $\hat{x}_1$. An error dynamic of SMO for $\hat{x}_1$ estimation is written as

$$\dot{e}_1 = a_1\left(e_L + e_2 - \left(V_{\mathrm{oc}} - \hat{V}_{oc}\right)\right) + \Delta x_1 - L_2 sgn(e_1) \quad (54)$$

Where $e_2 = (x_2 - \widehat{x_2})$. It is assume that the error between the actual V_{oc} and $\hat{V}_{oc}$ is an piecewise linear to e_1, hence it takes

$$V_{\mathrm{oc}} - \hat{V}_{oc} \approx me_1 \quad (55)$$

where m is a positive gain that evolved the slope of V_{oc} over SOC. Having (55) the (54) results

$$\dot{e}_1 = a_1(e_L + e_2 - me_1) + \Delta x_1 - L_2 sgn(e_1) \quad (56)$$

Similarly, the SMO model of

$$\dot{\hat{x}}_2 = -a_2\widehat{x_2} + b_1 I_{\mathrm{L}} + + \Delta x_2 + L_3 sgn(e_2) \quad (57)$$

Having a relation between three error terms

$$e_2 = \left\{\frac{L_2}{a_1}sgn(e_1)\right\} = \left[\frac{L_2}{a_1}sgn\left(\left\{\frac{L_1}{ma_2}sgn(e_L)\right\}_{eq}\right)\right]_{eq}, \quad (58)$$

the SMO model (57) results

$$\dot{\hat{x}}_2 = -a_2\widehat{x_2} + b_1 I_{\mathrm{L}} + L_3 sgn\left(\left[\frac{L_2}{a_1}sgn\left(\left\{\frac{L_1}{ma_2}sgn(e_L)\right\}_{eq}\right)\right]_{eq}\right) \quad (59)$$

For considered SOC problem, the SMO converges to the conditions $L_2 > |\Delta x_1|$ and $L_3 > |\Delta x_2|$

V. Simulation Results and Discussions

This section presents simulation results of SMO based Li-S cell SOC estimation. Simulation has performed under two different ECN model conditions and two different load conditions. Having constant current, simulation demonstrates the performance of Li-S cell SOC estimators under conventional load condition. To demonstrate performance of estimators under dynamic load condition, the mixed-amplitude current is considered.

Firstly, performance of SMO is studied under deterministic model and two different load conditions; constant and mixed-amplitude load current. For both load condition the SMO performs well when model is deterministic and it result is not presented here due to page limit. But result of deterministic model based SMO is much better and accurate than the perturbed model.

Secondly, performance of SMO for model with Q-uncertainty is studied and compared it to the EKF under two load conditions.

A. Constant Load Current

The current is constant, but added with a random noisy as Fig 6a, which is actual measured current of NASA data set [2]. For this input load current, the Li-S cell's output voltage is generated from ECN model (28). Fig 6b shows measured voltage when measurement noise is set to $R_a = 0.00001V^2$ In this case, the perturbation in the model is set to be Q_{soc}=0.0000003 and $Q_{vp} = 0.1V^2$.

The SMO and EKF use the measured voltage and input current, and estimate the SOC of Li-S battery. The subplot of Fig 6c compares the estimated SOC and true SOC. In Fig 6c, the black dotted, red solid line and blue dashed lines denote true SOC, EKF and SMO, respectively. This comparison plot exhibits that the performance of SMO as close as the true SOC from the beginning (100 percent SOC) to the depletion state (zero percent SOC), whereas the EKF does not. After 25 percent of the SOC the EKF diverges from the true SOC and is an unstable. Fig 6d shows the error in estimation by both EKF and SMO. The error of SMO is less than five percent through the discharge. On contrast to the SMO, the error of EKF is more than five percent in the discharging range 25 to zero percent though the EKF's error is less than five percent from 100 percent SOC to until 25.

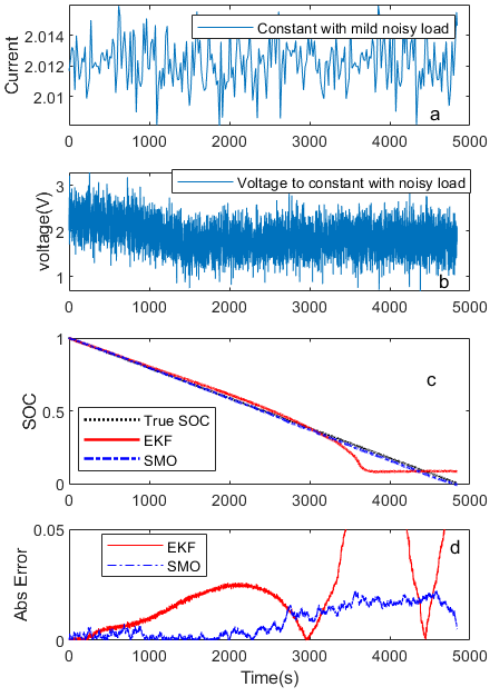

Fig.6 Results when load is constant: (a)voltage; (b) current; (b) voltage; (c) SOC estimated Vs true SOC (d) absolute error SMO vs EKF

B. *Mixed-Amplitude Pulse Load Current*

This subsection illustrates the performance of both SMO and EKF based SOC estimation of Li-S batteries when mixed –amplitude current is applied. On top of that, the model perturbation is set to be Q_{soc} =0.00001 and $Q_{vp} = 0.00001V^2$. Like previous case, the measurement noise is set to $R_a = 0.00001V^2$. Fig 7a and Fig 7b show the dynamic current and voltage of Li-S respectively.

Like constant current case, the SMO converges through the 100 percent SOC to zero percent, but the EKF starts diverges from beginning of the low-plateau around 73 percent SOC. Fig 7c illustrates the response of SMO and EKF when applied dynamic current. The red solid-line moves away from the true SOC, which is black dotted-line of Fig 7c. The red solid-line of Fig 7d shows that the absolute error by EKF is slowly increasing in low-plateau region because the poorly-observable low-plateau region. But the error by SMO is less than five percent in both high- and low-plateau.

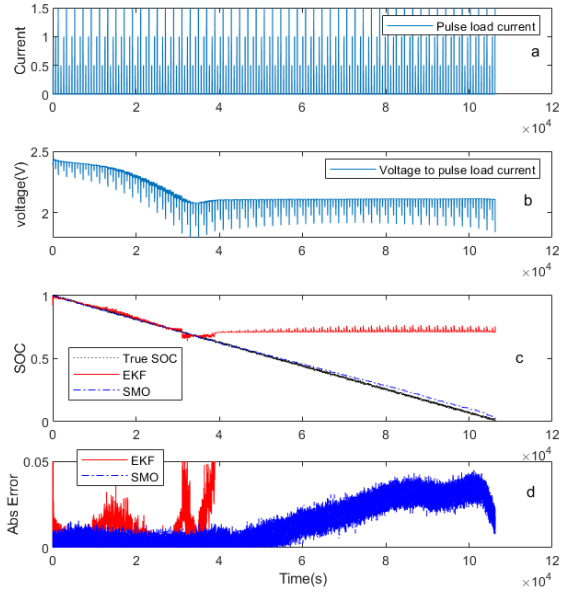

Fig.7 Results when load is mixed-amplitude pulses (a)pulse current; (b) voltage; (c) SOC estimated Vs true SOC, x_1; (d) absolute error SMO vs EKF.

VI. Conclusions and Future Works

After addressing modelling complexity, a sliding mode observer has been designed for SOC estimation of discharging Lithium-Sulfur battery cell under constant and mixed-pulse dynamic current. Thus, a literature gap on SMO based Li-S battery SOC estimation is fulfilled. The performance between SMO and conventional EKF has been compared. The SMO is much robust than the EKF when the model is heavily perturbed. The absolute error between estimated and true SOC is used to measure the accuracy of estimators. The SMO's error in accuracy is five percent through, whereas the EKF did not for considered dynamic load and perturbed Li-S battery model. Therefore the SMO based SOC estimator is highly recommended for the Li-S batteries that have Q-uncertainty. The future works include a study on robustness against initial SOC uncertainty and a design of dual SMO for state of health estimation of Li-S batteries.

Acknowledgment

The authors thank the Aerospace Technology Institute (ATI) and Innovate UK who funded this work under grants TS/P003818/1 and TS/R013780/1, and European commission grant 814471e.

References

[1] K. Propp, M. Marinescu, D. J. Auger, L. O'Neill, A. Fotouhi, K. Somasundaram, G. J. Offer, G. Minton, S. Longo, M. Wild and V. Knap, "Multi-temperature state-dependent equivalent circuit discharge model for lithium-sulfur batteries," *Journal of Power Sources*, vol.328, pp.289-299. Oct 2016. Dataset/s: 10.17862/cranfield.rd.c.3292031.

[2] S. Leutenegger, "Unmanned Solar Airplanes: design and algorithms for efficient and robust autonomous operation," Doctor of Sciences Dissertation, ETH Zurich, 2014.

[3] A. Fotouhi, D. J. Auger DJ, K. Propp, S. Longo, R. Purkayastha, L. O'Neill and S. Walus, "Lithium-Sulfur cell equivalent circuit network model parameterization and sensitivity analysis," *IEEE Transactions on Vehicular Technology*, vol. 66, no.9,pp. 7711-7721, 2017

[4] Propp, D. J. Auger, A. Fotouhi, S. Longo, V. Knap, "Kalman-variant estimators for state of charge in Lithium-sulfur batteries," *Journal of Power Sources*, vol. 343, pp. 254-267, March 2017.

[5] Chu Xu, Timothy Cleary, Daiwei Wang, Guoxing Li, Christopher Rahn, Donghai Wang, Rajesh Rajamani, Hosam K. Fathy, Online state estimation for a physics-based Lithium-Sulfur battery model, Journal of Power Sources, Volume 489, 2021, 229495, ISSN 0378-7753, https://doi.org/10.1016/j.jpowsour.2021.229495

[6] Propp, D. J. Auger, A. Fotouhi, M. Marinescu, V. Knap, and S. Longo, "Improved State of Charge Estimation for Lithium-Sulfur Batteries," *Journal of Energy Storage*, 2019, vol. 26, pp. 100943, 2019.

[7] A. Fotouhi, D. J. Auger, K. Propp and S. Longo, "Lithium-sulfur battery state-of-charge observability analysis and estimation," *IEEE* Transactions on Power Electronics, vol.33, no.7, pp. 5847-5859, 2018.

[8] N. Shateri, Z. Shi, D. J. Auger and A. Fotouhi, "Lithium-Sulfur Cell State of Charge Estimation Using a Classification Technique," in IEEE Transactions on Vehicular Technology. 2020 doi: 10.1109/TVT.2020.3045213.

[9] I. Kim, "A Technique for Estimating the State of Health of Lithium Batteries Through a Dual-Sliding-Mode Observer," in IEEE Transactions on Power Electronics, vol. 25, no. 4, pp. 1013-1022, April 2010, doi: 10.1109/TPEL.2009.2034966.

[10] G. Sethia, S. K. Nayak and S. Majhi, "An Approach to Estimate Lithium-Ion Battery State of Charge Based on Adaptive Lyapunov Super Twisting Observer," in *IEEE Transactions on Circuits and Systems I: Regular Papers*, vol. 68, no. 3, pp. 1319-1329, March 2021, doi: 10.1109/TCSI.2020.3044560

[11] A. Clemente, M. Montiel, F. Barreras, A. Lozano and R. Costa-Castelló, "Vanadium Redox Flow Battery State of Charge Estimation Using a Concentration Model and a Sliding Mode Observer," in *IEEE Access*, vol. 9, pp. 72368-72376, 2021, doi: 10.1109/ACCESS.2021.3079382

[12] Auger, Daniel; Fotouhi, Abbas; Longo, Stefano (2016): Simulink models from 'Multi-temperature state-dependent equivalent circuit discharge model for lithium-sulfur batteries. Cranfield Online Research Data Dataset. https://doi.org/10.17862/cranfield.rd.3507683.v1J. accesed on 17/08/21.

[13] B. Saha and K. Goebel (2007). "Battery Data Set", NASA Ames Prognostics Data Repository (http://ti.arc.nasa.gov/project/prognostic-data-repository), NASA Ames Research Center, Moffett Field, CA. accessed on 05 Dec 2021.